Lithuanian Journal of Physics, Vol. **50**, No. 1, pp. 7–15 (2010) doi:10.3952/lithjphys.50114

MAGNETOOPTICS OF OPAL CRYSTALS MODIFIED BY COBALT NANOPARTICLES

I. Šimkienė [a], A. Rėza [a], A. Kindurys [a], V. Bukauskas [a], J. Babonas [a], R. Szymczak [b], P. Aleshkevych [b], M. Franckevičius [c], and R. Vaišnoras [c]

[a] *Semiconductor Physics Institute, A. Goštauto 11, LT-01108 Vilnius, Lithuania*
E-mail: jgb@pfi.lt
[b] *Institute of Physics of the Polish Academy of Sciences, Lotników 32/46, PL-02668 Warsaw, Poland*
[c] *Vilnius Pedagogical University, Studentų 39, LT-08106 Vilnius, Lithuania*

Received 15 July 2009; accepted 19 March 2010

Optical and magnetooptical properties of opal photonic crystals modified by Co nanoparticles have been investigated by modulation spectroscopy technique in the visible spectral range from 400 to 800 nm. The Co nanoparticles of 1 to 8 nm in size were formed by means of chemical reduction reaction inside synthetic opal crystals composed of regularly close-packed SiO_2 spheres of diameter 250–300 nm. As it was estimated from the spectral shift of the stop band of photonic crystals, Co nanoparticles occupied up to several percent of void volume in opal crystal lattice. In the Faraday configuration, external magnetic field induced the change in optical transmission normalized to sample thickness 1 cm and magnetic field 1 T equal to 0.10–0.35 for Co-modified opal crystals in the spectral range under consideration. The fabricated hybrid structures can be considered as a possible prototype of magnetophotonic crystals.

Keywords: magnetophotonic crystals, modulation spectroscopy

PACS: 42.70.Qs, 78.20.Ls

1. Introduction

The possibility to form the photonic band gap has invoked a great interest to photonic crystals (PCs) [1] such as synthetic opals, which possess the photonic band gap in visible spectral range. The presence of magnetic component in photonic crystals leads to extension of functionality of hybrid samples and fabrication of magnetophotonic crystals (MPCs) [2]. MPCs were developed on the basis of opal-type structures infiltrated with various magnetic compounds such as $(Bi,Y)Fe_5O_{12}$ and Tb-Ga garnets [3–5], magnetite Fe_3O_4 [6–8], magnetic fluids $Dy(NO_3)_2$ [9] and iron porphyrin FeTPPS [10], cobalt ferrite $CoFe_2O_4$ [11], and BiNi [12]. At the present state of studies, the current problem is a search of prospective materials for fabrication of MPCs and determination of the main regularities in magnetooptical properties of these hybrid structures. However, until recently magnetooptical (MO) properties of 3D MPCs have not been extensively studied.

In this work the optical and magnetooptical properties of hybrid structures composed of synthetic bulk opal crystals with Co nanoparticles (NPs) have been investigated. The main goal was to develop the fabrication procedure for hybrid samples and to correlate the optical and magnetooptical properties with the sample structure and magnetic characteristics.

2. Experiment

The bulk opal crystals were synthesized (OPALON, Moscow) by gravitational sedimentation technique from monodispersed colloid solutions of SiO_2 spheres of diameter in the 250–300 nm range. In bulk synthetic sample the SiO_2 spheres were regularly spaced in fcc symmetry with the growth plane (111). The platelet samples of thickness 0.5–1.0 mm with the sides parallel to crystallographic plane (111) were cut and polished. In the sample surface plane (Fig. 1(a)) the domains of $\sim$10 μm in size were observed with point and line defects typical of solid state structures.

The Co NPs were formed inside the synthetic bulk opal samples by chemical reduction technique [13]. The presence of silanol groups on the surface of SiO_2 spheres [14] favours the formation of metal NPs. As precursor, water solutions of $CoCl_2{\cdot}6H_2O$ of concentration 0.25–0.30% (samples OP1G, OP1F2, OP1l) and

ISSN 1648-8504

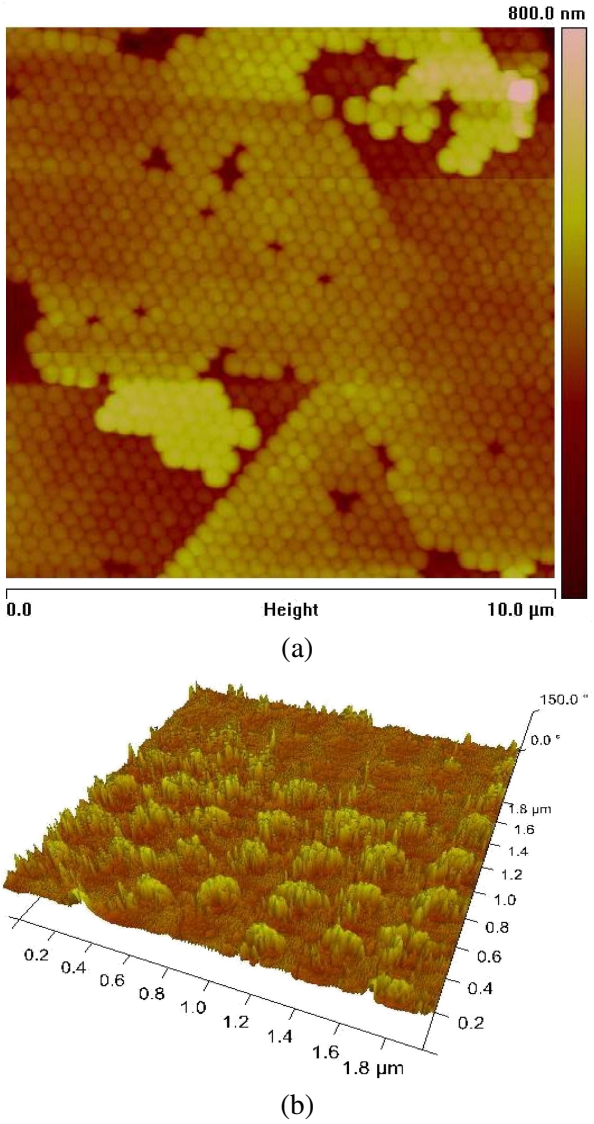

Fig. 1. (a) AFM image of pure opal (sample M4c) and (b) MFM image of Co-modified (sample M8c) synthetic opal.

1% (sample M4c) were used. The Co ions were reduced with ethanol solutions of $NaBH_4$ of concentration from 0.3 (OP1F) to 1.0% (M4c, OP1G) varying in dependence on the concentration of Co salt solutions. The reduction time varied from 10 min (M4c) to 1 h (OP1G, OP1F). The ions Co^{2+} were reduced to metallic Co^0 along the following reactions [15]:

$$2CoCl_2 + 4NaBH_4 + 9H_2O \rightarrow$$

$$Co_2B + 4NaCl + 12.5H_2 + 3B(OH)_2\,,$$

$$4Co_2B + 3O_2 \rightarrow 8Co + 2B_2O_3\,.$$

The reaction process underwent very quickly indicating spontaneous formation of Co seeds. It should be emphasized that in nonaqueous solution Co metal NPs are formed because the nonaqueous solvent, like ethanol, acts as a ligand L according to the following reaction [16]:

$$Co^{2+} + 2NaBH_4 + nL \rightarrow (L)_nCo(BH_4)_2 + 2Na^+\,,$$

$$(L)_nCo(BH_4)_2 \rightarrow Co + H_2 + B_2H_6 + nL\,.$$

The Co metal NPs were formed inside bulk opal samples by immersion into solution. After immersion procedure, the samples were carefully washed in hexane and dried for 0.5–1.0 h at 100 °C.

The structural studies have been carried out by means of scanning probe microscope (SPM) Dimension 3100 / Nanoscope IVa from Veeco Metrology Group. The structure of sample surfaces was visualized in a tapping mode. The distribution of magnetic moments in the lateral plane was investigated by magnetic force microscopy (MFM) technique with magnetized Co/Cr-coated tips.

The magnetic properties of hybrid samples were studied in a wide temperature range (5–300 K) in magnetic fields up to 5 T making use of magnetometer Quantum Design. The temperature dependence of magnetic moment was investigated in both field-cooled (FC) and zero field-cooled (ZFC) regimes.

The optical properties of hybrid sample were studied in visible spectral range in the vicinity of the stop band of opal PCs. The measurements have been carried out by means of the set-up based on monochromator MDR-2 in the transmission and reflectance modes at various angles of light incidence. The divergence of the incident light beam was $\sim 1^\circ$. The light transmitted or reflected from the sample was collected by fibre optical system with the angle aperture equal to 1.27°. The incidence/reflection angle was scanned with a minimal step equal to $4'$.

The MO spectra were investigated in the 400–700 nm range by means of photometric spectroscopic ellipsometer with photoelastic modulator (PEM) of light polarization operating at the frequency $\Omega = 30$ kHz. The standard measurements were carried out in the PCSA – *P*(olarizer)-*C*(ompensator)-*S*(ample)-*A*(nalyzer) – configuration with PEM as compensator inducing the phase difference $\delta_C = A_0 \sin \Omega t$ (A_0 is the modulation amplitude) between the normal components of polarized light. Analysis of detector signal depends essentially on the polarization state of normal waves propagating in the sample [17]. It is reasonable to assume that in

Faraday configuration cubic opal samples under consideration possess the circular birefringence CB

$$\mathrm{CB} = 2\pi d\,\frac{n_- - n_+}{\lambda}\,, \tag{1}$$

where $n_{-,+}$ is refraction index for circularly left $(-)$ and right $(+)$ polarized light of wavelength λ and d is the sample thickness. The CB is directly related to the magnetic Faraday rotation [18].

In the region of the stop band of PC the particular features of ellipsometric parameters can be considered [19] as pseudoabsorption band due to the Bragg diffraction. Therefore, in the studies of MO effects the manifestation of magnetic circular dichroism CD can be expected in this spectral range:

$$\mathrm{CD} = (K_- - K_+)\,d = \Delta K\,d\,, \tag{2}$$

where $K_{-,+}$ is absorption coefficient for circularly polarized light. In particular, at azimuth angles of optical elements at $P = A = C - P = \pi/4$, the signal at fundamental and double modulation frequency is

$$I_\Omega = 2J_1(A_0)\,\sin 2\Psi\,\sin\Delta\,, \tag{3}$$

$$I_{2\Omega} = 2J_2(A_0)\,\sin 2\Psi\,\cos\Delta\,, \tag{4}$$

where $J_m(A_0)$ is the first kind mth order Bessel function and $J_0(A_0) = 0$ at optimal modulation amplitude, Ψ and Δ are ellipsometric parameters [17].

However, in some bulk opal samples the birefringence induced by residual strain was observed [20] leading to the presence of linear birefringence LB. In addition, in opal crystals intrinsic optical anisotropy was detected [21] in the region of the stop band. As a result, in magnetic field, the bulk opal crystal should correspond to a gyro-anisotropic structure [22], the polarization properties of which become quite complicated. The ellipticity ε of the normal waves (where $\tan\varepsilon = b/a$, a and b are the major and minor semiaxes of polarization ellipse, respectively) in transparent gyro-anisotropic media is caused by the ratio [17]

$$\tan 2\varepsilon = \frac{G}{\bar{n}\,\Delta n}\,, \tag{5}$$

where G is gyration [18], $\bar{n}$ is the average refraction index, and Δn is linear birefringence. According to the superposition principle [18], the phase difference between the normal waves propagating in gyro-anisotropic crystal is determined by two contributions due to CB and LB:

$$\Delta = \frac{2\pi d}{\lambda}\sqrt{(\Delta n)^2 + \left(\frac{G}{\bar{n}}\right)^2}\,. \tag{6}$$

In the case of small gyration ($G \ll \bar{n}\,\Delta n$), at the orientation of optical elements $P = 0$, $C - P = \pi/4$, $A = \pi/2$, the ellipticity of normal waves can be determined [17] from

$$\frac{G}{\bar{n}\,\Delta n} = -\frac{I_\Omega}{I_{2\Omega}}\,\frac{J_2(A_0)}{2J_1(A_0)} \tag{7}$$

at the wavelength corresponding to interference extremum, i. e., at $\sin(\Delta/2) = 1$. It should be emphasized that the electromagnetic waves transmitted through 1D MPC become elliptically polarized in the region of stop bands, even in non-absorbing case and at $G = 0$.

In the present investigations, the signal at the fundamental frequency I_Ω in the experimental geometry PCS and PCSA has been measured for determination of MCD and effective magnetic birefringence, respectively. The Faraday rotation was measured at signal of double frequency $I_{2\Omega}$ in PCSA geometry with azimuth angle $P - A = \pi/4$. The linear dichroism LD was also studied at registration of the fundamental frequency signal I_Ω in the PC($\lambda/4$)S geometry (where $\lambda/4$ is the quarter-wavelength phase plate).

Though several mechanisms contribute to MO effects, the measured signal was always related to the magnetic field-induced changes. The final MO effect was determined as the difference between two signals obtained at external magnetic field of opposite directions:

$$I_\Omega = \frac{1}{2}\left(I_\Omega^{+B} - I_\Omega^{-B}\right), \tag{8}$$

where I_Ω^{+B} and I_Ω^{-B} are the signals measured in the Faraday configuration for a constant magnetic field along the light beam and in opposite direction, respectively.

3. Results and discussion

The structural studies have confirmed the presence of Co NPs in hybrid opal samples. As an illustration, Fig. 1(b) presents the magnetic force microscope (MFM) phase image, in which the difference in magnetic properties of hybrid sample components is clearly revealed. As is seen, the magnetic clusters composed of Co NPs are formed on SiO_2 spheres and in the voids between them. However, the size of Co NPs is difficult to estimate from MFM/AFM images because of the roughness of opal surface composed of SiO_2 spheres. Therefore, the Co NPs on Si surface were prepared by the same technology as that used for their formation inside bulk opal samples. As seen from Fig. 2, two types

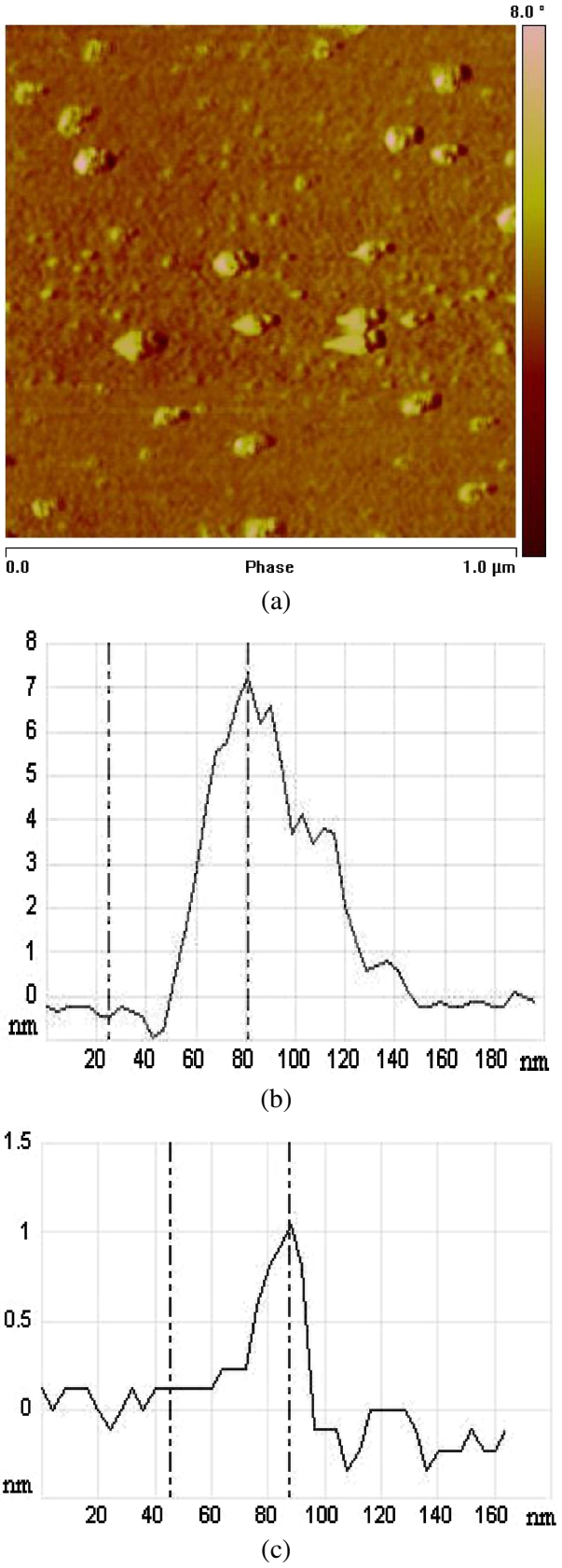

Fig. 2. AFM images of Co nanoparticles on Si. (a) AFM phase image of the Si surface with Co nanoparticles and cross-section profiles of (b) larger and (c) smaller Co nanoparticles in height image.

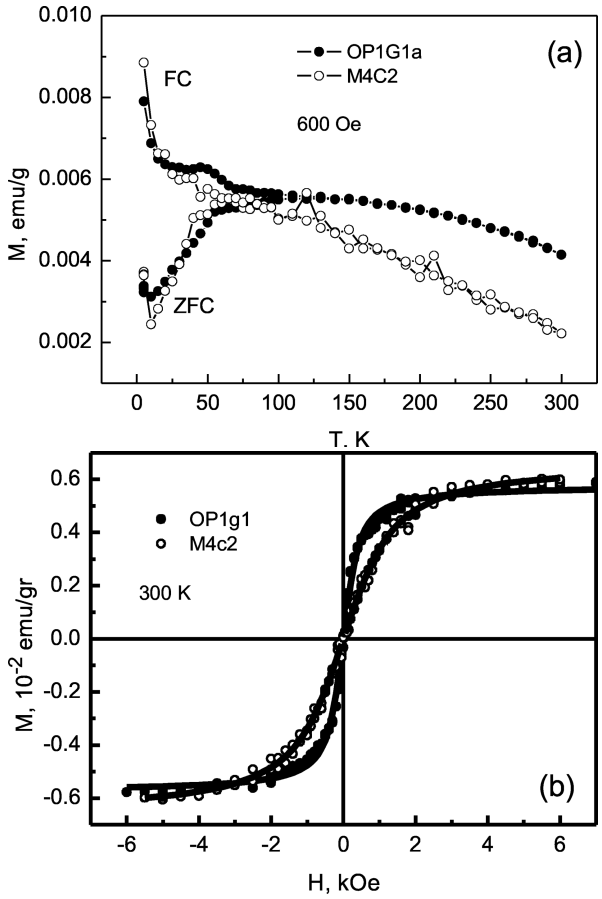

Fig. 3. (a) Temperature and (b) field dependences of magnetization for two Co-modified opal samples. In (b) experimental data (points) and Langevin fitting (curves) are shown.

of Co NPs, larger and smaller, have been observed. The presence of magnetic clusters is explicitly detected in the phase image (Fig. 2(a)). It should be noted that in AFM height image, the profile of NPs in lateral plane is partially distorted because of the tip size, which is of order of 10–20 nm. For this reason, the size of Co NPs can be estimated more reliably from their height. From the analysis of cross-sections in height images (Fig. 2(b, c)) it follows that the size of Co NPs is of order of 1 and 8 nm for smaller and larger particles, respectively.

As is well known [13], physical properties of metal NPs fabricated by chemical reduction technique depend strongly on the formation conditions, which hence determine the morphology, chemical composition, and crystal structure of NPs. The investigations of temperature and field dependence of magnetization of hybrid opal samples have revealed the correlation between the magnetic properties and formation technology of Co NPs. Figure 3 illustrates the results of magnetic studies for two different samples of Co-modified synthetic bulk opal crystals. It should be noted that the diamagnetic contribution of opal matrix has been taken into

account in the estimation of the total magnetic moment of hybrid sample. As seen from Fig. 3(a), the blocking temperature $T_{\rm b}$, determined as the temperature at which the ZFC and FC curves start to separate and ZFC data show a maximum in the temperature scale, is higher for sample OP1G1a than that for sample M4c2. The difference in $T_{\rm b}$ value should be related to the average size of Co NPs. It could be noted that $T_{\rm b} = 150$ K was determined [23] for the system of silica-coated magnetite/maghemite nanoparticles of core diameter 30 nm.

The field dependence of magnetization M is well fitted by Langevin function, which has been previously used [24] for interpretation of superparamagnetism of Co NPs. The presence of Co NPs of two different sizes ($i = 1, 2$) was taken into account:

$$M = \chi H + \sum_i M_{\rm sat}^{(i)} \left(\frac{1}{\tan x_i} - \frac{1}{x_i} \right), \qquad (9)$$

where χ is magnetic susceptibility, $M_{\rm sat}^{(i)}$ is the saturation moment, $x_i = \mu_i H/(k_{\rm B}T)$, μ_i is the effective moment of a unit magnetic cell, and $k_{\rm B}$ is the Boltzmann constant. The diameter d_i of Co NPs was estimated assuming that interaction inside NP is the same as in bulk Co:

$$d_i = \left(\frac{6\mu_i}{\pi M_{\rm s}} \right)^{1/3}, \qquad (10)$$

where $M_{\rm s}$ is spontaneous magnetization.

The analysis of the magnetic data has shown that at 300 K the Co NPs in opal can be considered as the system of non-interacting superparamagnetic clusters with ferromagnetic interaction inside cluster. It should be noted that the diamagnetic contribution (χ) of opal matrix at $T = 300$ K was measured separately and found to be $-4.564{\cdot}10^{-7}$ emu/(g Oe). The corresponding diamagnetic contribution χH of opal matrix was subtracted from experimental curves in Fig. 3(b). In the investigated series of Co-modified opal samples, it was estimated from the field dependence that total magnetic moment consists of magnetic moments' clusters, grouped around two dominant sizes. For example, the average moments of magnetic clusters are $13{\cdot}10^3$ $\mu_{\rm B}$ (where $\mu_{\rm B}$ is Bohr magneton) and $5{\cdot}10^3$ $\mu_{\rm B}$ for M4c2 sample, $29{\cdot}10^3$ $\mu_{\rm B}$ and 170 $\mu_{\rm B}$ for OP1G1a sample, whereas the number of clusters $N = M_{\rm sat}/\mu$ is correspondingly $2.3{\cdot}10^{13}$ and $1.1{\cdot}10^{14}$ for M4c2 sample, $2.1{\cdot}10^{13}$ and $1.4{\cdot}10^{16}$ for OP1G1a sample. Assuming the spherical shape of clusters and spontaneous magnetization within clusters to be $M_{\rm s} = 1422$ Gs [25], the two dominant sizes of Co NPs were estimated to be 5.4 and 3.9 nm in M4C2 sample, 7.1 and 1.3 nm in OP1G1a sample for larger and smaller particles, respectively. The values are in a reasonable agreement with those evaluated from structural investigations of Co NPs on Si surface. Some correlation between the size of Co NPs and magnetization characteristic should be noted.

At low temperatures ($T < 60$ K) the magnetization shows hysteresis loop with coercivity growing up to 600 Oe and 740 Oe at $T = 5$ K for M4c2 and OP1G1a samples, respectively. The remnant magnetization grew up to $\sim 0.5{\cdot}10^{-2}$ emu/g at $T = 5$ K in both samples. It should be noted that magnetization shows no hysteresis loop at room temperature in the present samples, however in the composite system of Co NPs implanted in SiO_2 matrix the hysteresis loop was observed even at 300 K at high ion doses $\sim 1{\cdot}10^{17}$ ions/cm^2 [26]. The coercivity fields due to ferromagnetic interaction in SiO_2-coated Co NPs of diameter $\sim$25 nm were found to be dependent on technology, mainly on calcination temperature, which has influenced both the properties and structure [27].

The presence of Co NPs in hybrid opal PC influences significantly the optical properties of Co-modified opal crystals. On the one hand, the contribution due to surface plasmon resonance (SPR) [28] of metal NPs could be expected. The enhancement of MO effects and particular features has been predicted in the vicinity of SPR in granular magnetic materials [29]. The MO effects were found to be influenced by the size and shape of metal NPs. However, for Co NPs even in the SiO_2 matrix, the SPR peak manifests itself at $\lambda < 300$ nm [30], i. e., significantly below the stop band of opal PC under consideration. On the other hand, the Faraday rotation and other MO effects were shown [31] to change considerably at the stop band for both 1D and 3D MPCs. The presence of metal component influences the average refraction index of hybrid sample $n_{\rm eff}$ and hence the spectral position λ_m of the stop band due to the Bragg diffraction of mth order [1]. In the case of close-packed SiO_2 spheres

$$\lambda_m = \frac{2a}{m} \sqrt{n^2(\lambda) - \sin^2 \phi}, \qquad (11)$$

where $a = D\sqrt{2/3}$ is the distance between the (111) crystallographic planes in fcc symmetry lattice, D is the diameter of SiO_2 sphere, and ϕ is the angle of light incidence with respect to the surface normal. The effective

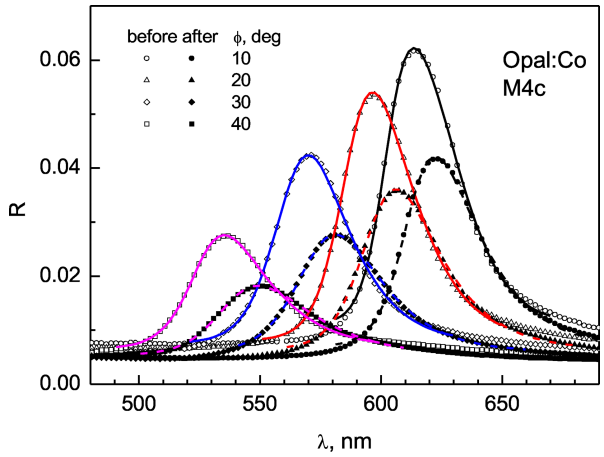

Fig. 4. Experimental (points) reflection spectra approximated by asymmetric lines (curves) at various angles of light incidence for opal crystal (sample M4c) before and after formation of Co nanoparticles inside opal lattice.

dielectric function of hybrid sample $\varepsilon_{\text{eff}} = n_{\text{eff}}^2$ can be estimated in the approximation of effective media [28]:

$$\varepsilon_{\text{eff}} = \sum_i f_i \varepsilon_i \,, \tag{12}$$

where f_i is the volume fraction of ith component with dielectric function ε_i. In the case of spheres closely packed in fcc lattice, $f_{\text{sph}} = 0.74$ and $f_{\text{v}} = 0.26$ for spheres and voids between them, respectively.

Figure 4 shows the reflection spectra for bare and Co-modified opal bulk crystal sample at various angles of light incidence. The spectral dependence of reflection coefficient R was approximated by asymmetric line

$$y = y_0 + A\left[1 + \exp\left(-\frac{x - x_c + \omega_1/2}{\omega_2}\right)\right]^{-1} \times \left\{1 - \left[1 + \exp\left(-\frac{x - x_c + \omega_1/2}{\omega_3}\right)\right]^{-1}\right\}, \tag{13}$$

where A and x_c is the amplitude and spectral position of the line and ω_1, ω_2, ω_3 are the halfwidth of the line and asymmetry parameters.

As seen from Fig. 4, the reflection peak is shifted to longer wavelengths in hybrid samples as compared to bare opal samples. The shift increases from 7 to 14 nm for light incidence angles varying from 10 to 40°. The difference in the shift for various incidence angles can be caused by non-homogeneity of the synthetic bulk opal crystal and due to non-homogeneous distribution of Co NPs into the sample depth. However, making use of (11), (12), and Co optical constants [32], the ε_{eff} value for hybrid sample can be estimated. In this approximation it was found that Co NPs occupy 0.5–1.0% of voids in the samples under investigation.

The presence of even such a low concentration of Co ions results in some reliably observed MO effects of hybrid Co-modified opal samples. Figures 5 and 6 illustrate typical MO spectra with specific features developed in the region of PC stop band. In Fig. 5(a) the MCD spectrum $(\Delta K_C d)_{\text{MO}}$ measured in PCS geometry is shown along with the optical transmission spectrum. As is seen, in the region of stop band the MCD is strongly enhanced. The maximal signal is $\sim 0.44 \cdot 10^{-2}$ for the sample OP11 ($d = 0.75$ mm) in magnetic field of 300 mT. In MCD spectrum inside the stop band, the fine structure detected that has been predicted theoretically [33] for 1D MPC. The magnitude of observed MCD is similar to that for fcc opal films modified with Fe_3O_4 [7]. However, for comparison of the absolute values, the difference in sample characteristics should be taken into account.

The results of the studies of magnetic Faraday rotation are depicted in Fig. 5(b) for the same Co-modified opal sample OP11 as in Fig. 5(a). The Faraday rotation is of order of 1 deg with enhanced value at the stop band.

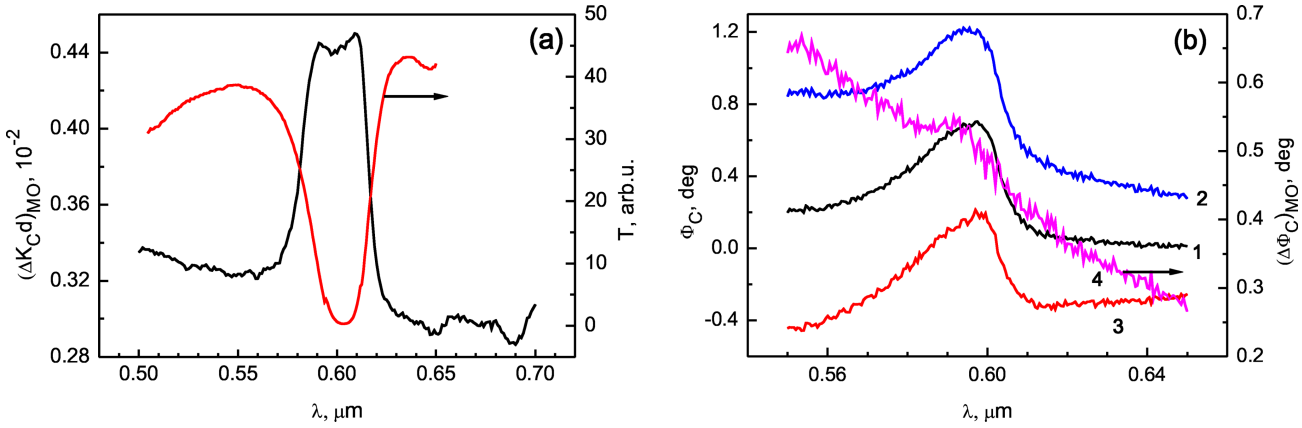

Fig. 5. (a) MCD, transmission T, and (b) Faraday rotation spectra of sample OP11 of Co-modified opal crystal immersed in isopropyl alcohol. In (b) the spectra are shown for magnetic field 0 (*1*), +350 mT (*2*), −350 mT (*3*), and resulting MO effect (*4*).

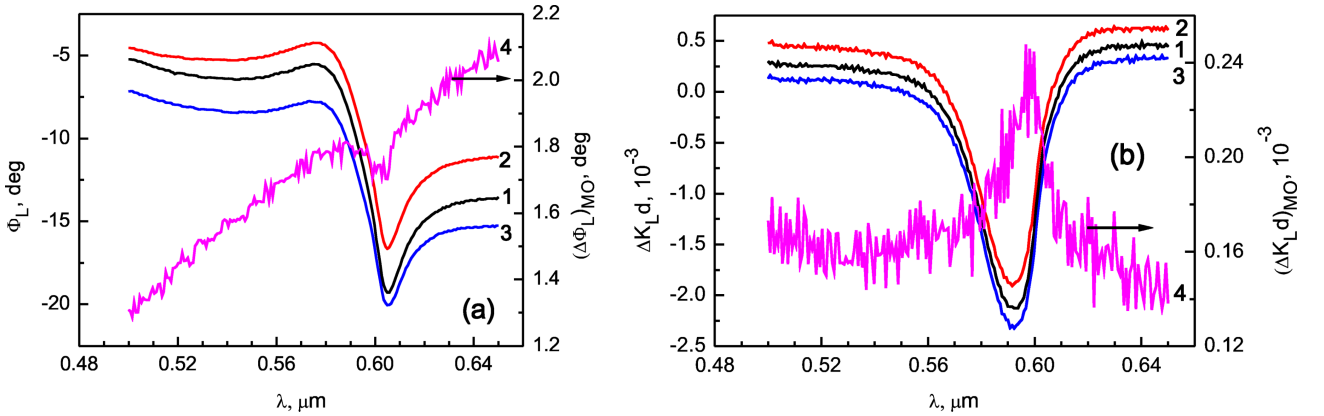

Fig. 6. Spectra of magnetic (a) LB and (b) LD in sample OP11 of Co-modified opal crystal immersed in isopropyl alcohol. The spectra are measured in magnetic field 0 (*1*), +350 mT (*2*), −350 mT (*3*), and resulting MO effect (*4*).

Note the fine structure of the $I_{2\Omega}$ signal at the stop band in zero magnetic field. It is reasonable to assume that this signal is contributed by the linear anisotropy (LB and LD) in opal crystals [17]. It should be noted that the particular features were not observed in nanocomposite materials of Co NPs in SiO_2 matrix in the corresponding spectral range [26]. Therefore, the enhancement of Faraday rotation in the vicinity of the stop band (Fig. 5(b)) can be attributed to particular feature of opal PC. A similar enhancement of Faraday rotation was observed in opal-magnetite composite [34].

The effective LB and LD spectra are presented in Fig. 6. The shape of LB spectra is analogues to that for Faraday rotation. The observed signal was considered as magnetic field-induced ellipticity of normal waves due to the phase difference $(\Delta\Phi_L)_{\mathrm{MO}}$ (Fig. 6(a)). In this approximation in a series of Co-modified opal crystals, the external magnetic field of order of 350 mT induced the phase difference of electromagnetic waves varying from circa 35 to 60 deg/(cm T) in the spectral range from 700 to 400 nm resulting in a corresponding change 0.10–0.35 in optical transmission.

It should be noted that in samples of investigated series with thickness of order of 0.5 mm in magnetic field of ∼300 mT, a weak magnetic linear dichroism of order of $1{\cdot}10^{-4}$ was also observed (Fig. 6(b)). The magnetic LD increased two times near the stop band.

Summarizing, the 3D MPCs of bulk synthetic opal with Co particles of nanometric size were successfully prepared. The characteristics of Co NP were directly determined by SPM measurements. The magnetic properties of hybrid samples have shown that the Co NP correspond to the superparamagnetic system of non-interacting clusters at 300 K whereas magnetic interaction was significant at lower temperatures with a typical hysteresis observed at 5 and 25 K. The stop band was shown to be dependent on the concentration of Co NPs. From the shift of the stop band the Co NP was determined to occupy up to 2% of the voids in opal structure. The MO studies have shown that external magnetic field effectively influenced the optical transmission properties of hybrid Co-modified opal samples.

Acknowledgement

Support from the Lithuanian State Science and Studies Foundation (project T-36/08) is gratefully acknowledged.

References

[1] S.G. Johnson and J.D. Joannopoulos, *Photonic Crystals: Road from Theory to Practice* (Springer, 2003).

[2] M. Inoue, H. Uchida, K. Nishimura, and P.B. Lim, Magnetophotonic crystals – a novel magneto-optic material with artificial periodic structures, J. Mater. Chem. **16**, 678–684 (2006).

[3] R. Fujikawa, A.V. Baryshev, A.B. Khanikaev, H. Uchida, P.B. Lim, and M. Inoue, Fabrication and optical properties of three-dimensional magnetophotonic heterostructures, IEEE Trans. Magn. **42**, 3075–3077 (2006).

[4] A.V. Baryshev, T. Kodama, K. Nishimura, H. Uchida, and M. Inoue, Three-dimensional magnetophotonic crystals based on artificial opals, J. Appl. Phys. **95**, 7336–7338 (2004).

[5] R. Fujikawa, A.V. Baryshev, H. Uchida, P.B. Lim, and M. Inoue, Fabrication of three-dimensional magnetophotonic crystals: Opal thin films filled with Bi:YIG, J. Magn. **11**, 147–150 (2006).

[6] V.V. Pavlov, P.A. Usachev, R.V. Pisarev, D.A. Kurdyukov, S.F. Kaplan, A.V. Kimel, A. Kirilyuk, and Th. Rasing, Enhancement of optical and magneto-optical effects in three-dimensional opal/Fe_3O_4 mag-

netic photonic crystals, Appl. Phys. Lett. **93**, 072502 (2008).

[7] V.V. Pavlov, P.A. Usachev, R.V. Pisarev, D.A. Kurdyukov, S.F. Kaplan, A.V. Kimel, A. Kirilyuk, and Th. Rasing, Optical study of three-dimensional magnetic photonic crystals opal/Fe_3O_4, J. Magn. Magn. Mater. **321**, 840–842 (2009).

[8] T. Kodama, K. Nishimura, A.V. Baryshev, H. Uchida, and M. Inoue, Opal photonic crystals impregnated with magnetite, Phys. Status Solidi B **241**, 1597–1600 (2004).

[9] C. Koerdt, G.L.J.A. Rikken, and E.P. Petrov, Faraday effect of photonic crystals, Appl. Phys. Lett. **82**, 1538–1540 (2003).

[10] A. Rėza, I. Šimkienė, G.J. Babonas, R. Vaišnoras, D. Kurdyukov, and V. Golubev, Magnetic circular dichroism of opal crystals infiltrated with iron porphyrin, Lithuanian J. Phys. **48**, 319–323 (2008).

[11] X. Xu, S.A. Majetich, and S.A. Asher, Mesoscopic monodisperse ferromagnetic colloids enable magnetically controlled photonic crystals, J. Am. Chem. Soc. **124**, 13864–13868 (2002).

[12] A. Gupta, A.Yu. Ganin, P. Sharma, V. Agnihotri, L.M. Belova, K.V. Rao, M.E. Kozlov, A.A. Zakhidov, and R.H. Baughman, Synthetic magnetic opals, Pramana **58**, 1051–1059 (2002).

[13] H. Bönnemann and R.M. Richards, Nanoscopic metal particles – synthetic methods and potential applications, Eur. J. Inorg. Chem. **2001**, 2455–2480 (2001).

[14] H. Hofmeister, P.-T. Miclea, and W. Mörke, Metal nanoparticle coating of oxide nanospheres for core-shell structures, Part. Part. Syst. Char. **19**, 359–365 (2002).

[15] G.N. Glavee, K.J. Klabunde, C.M. Sorensen, and G.C. Hadjipanayis, Borohydride reduction of cobalt ions in water. Chemistry leading to nanoscale metal, boride or borate particles, Langmuir **9**, 162–169 (1993).

[16] C. Petit and M.P. Pileni, Physical properties of self-assembled nanosized cobalt particles, Appl. Surf. Sci. **162–163**, 519–528 (2000).

[17] G. Babonas and G. Pukinskas, *Issledovanie opticheskikh i magnitoopticheskikh svoistv poluprovodnikov metodom spektral'noi ellipsometrii (Studies of Optical and Magnetooptical Properties of Semiconductors by Modulation Spectroscopy Technique)*, preprint No 23 (Semiconductor Physics Institute, Vilnius, 1988) [in Russian].

[18] J.F. Nye, Physical *Properties of Crystals: Their Representation by Tensors and Matrices* (Oxford University Press, 2000).

[19] A. Reza, R. Tamasevicius, J. Babonas, Z. Balevičius, V. Vaicikauskas, V. Golubev, and D. Kurdyukov, Ellipsometric studies of opal crystals, Phys. Status Solidi C **5**, 1391–1394 (2008).

[20] J. Sabataityte, I. Simkiene, G.-J. Babonas, A. Reza, M. Baran, R. Szymczak, R. Vaisnoras, L. Rasteniene, V. Golubev, and D. Kurdyukov, Physical studies of porphyrin-infiltrated opal crystals, Mater. Sci. Eng. C **27**, 985–989 (2007).

[21] A. Rėza, R. Vaišnoras, C. Lopez, D. Golmayo, and J. Babonas, Optical anisotropy of synthetic opals, in: *38-oji Lietuvos nacionalinė fizikos konferencija, Programa ir pranešimų tezės, Vilnius, 2009 m. birželio 8–10 d. (38th Lithuanian National Conference in Physics, Program and Abstracts, June 8–10, 2009)* (Vilnius, 2009) p. 250.

[22] G.A. Babonas and A.A. Reza, Izmerenie piezogiratsionnykh konstant kubicheskikh kristallov (Measurements of piezogyration constants in cubic crystals), Kristallografiya [Sov. Phys. Crystallogr.] **27**, 932–935 (1982) [in Russian].

[23] V. Salgueirino-Maceira, M.A. Correa-Duarte, M. Spasova, L.M. Liz-Marzan, and M. Farle, Composite silica spheres with magnetic and luminescent functionalities, Adv. Funct. Mater. **16**, 509–514 (2006).

[24] Y.-W. Zhao, R.K. Zheng, X.X. Zhang, and J.Q. Xiao, A simple method to prepare uniform Co nanoparticles, IEEE Trans. Magn. **39**, 2764–2766 (2006).

[25] C.M. Sorensen, Magnetism, in: *Nanoscale Materials in Chemistry*, ed. J.K. Klabunde (Wiley–Interscience, New York, 2001) pp. 169–220.

[26] I.S. Edelman, O.V. Vorotynova, V.A. Seredkin, V.N. Zabluda, R.D. Ivantsov, Yu.I. Gatiyatova, V.F. Valeev, R.I. Khaĭbullin, and A.L. Stepanov, Magnetic and magneto-optical properties of ion-synthesized cobalt nanoparticles in silicon oxide, Phys. Solid State **50**, 2088–2094 (2008).

[27] M. Wu, Y.D. Zhang, S. Hui, T.D. Xiao, S. Ge, W.A. Hines, and J.I. Budnick, Structure and magnetic properties of SiO_2-coated Co nanoparticles, J. Appl. Phys. **92**, 491–495 (2002).

[28] U. Kreibig and M. Vollmer, *Optical Properties of Metal Clusters* (Springer, Berlin, 1995).

[29] T.K. Xia, P.M. Hui, and D. Stroud, Theory of Faraday rotation in granular magnetic materials, J. Appl. Phys. **67**, 2736–2741 (1990).

[30] O. Yeshchenko, I. Dmitruk, A. Alexeenko, A. Dmitruk, and V. Tinkov, Optical properties of sol-gel fabricated Co/SiO_2 nanocomposites, Physica E **41**, 60–65 (2008).

[31] V.A. Kosobukin, Optics of circularly polarized light waves in one-dimensional magneto-photonic crystals: Theory, Solid State Commun. **139**, 92–96 (2006).

[32] *Landolt-Börnstein. Numerical Data and Functional Relationships in Science and Technology*, vol. 15, subvolume b, "Optical properties of pure metals and binary alloys" (Springer-Verlag, Berlin, 1985).

[33] M. Inoue, K. Arai, T. Fujii, and M. Abe, Magneto-optical properties of one-dimensional photonic crystals

composed of magnetic and dielectric layers, J. Appl. Phys. **83**, 6768–6770 (1998).

[34] A.V. Baryshev, T. Kodama, K. Nishimura, H. Uchida, and M. Inoue, Magneto-optical properties of three-dimensional magnetophotonic crystals, IEEE Trans. Magn. **40**, 2829–2831 (2004).

OPALO KRISTALŲ SU Co NANODALELĖMIS MAGNETOOPTIKA

I. Šimkienė [a], A. Rėza [a], A. Kindurys [a], V. Bukauskas [a], J. Babonas [a], R. Szymczak [b], P. Aleshkevych [b], M. Franckevičius [c], and R. Vaišnoras [c]

[a] *Puslaidininkių fizikos institutas, Vilnius, Lietuva*
[b] *Lenkijos MA Fizikos institutas, Varšuva, Lenkija*
[c] *Vilniaus pedagoginis universitetas, Vilnius, Lietuva*

Santrauka

Taikant moduliacinės spektroskopijos metodiką, tirti opalo fotoninių kristalų su Co nanodalelėmis optiniai ir magnetooptiniai spektrai regimojo spektro srityje nuo 400 iki 800 nm. Sintetiniuose opalo kristaluose, sudarytuose iš glaudžios sanklodos tvarka išsidėsčiusių 250–300 nm skersmens SiO_2 sferų, cheminės redukcijos reakcijose buvo suformuotos nuo 1 iki 8 nm dydžio Co nanodalelės. Iš fotoninio kristalo užtvarinės juostos poslinkio spektre nustatyta, kad Co nanodalelės užpildo kelis procentus opalo kristalo gardelės ertmių. Faradėjaus konfigūracijos opalo kristaluose su Co nanodalelėmis išorinis magnetinis laukas tirtoje spektro srityje sukelia optinio pralaidumo pokytį. Esant 1 cm storio bandiniui ir 1 T magnetiniam laukui, jis lygus 0,10–0,35. Pagaminti hibridiniai dariniai gali būti nagrinėjami kaip magnetofotoninių kristalų prototipai.